Accurate calculation of mutual inductance and magnetic fields in a birdcage coil

Patrice Boissoles, Gabriel Caloz

HAL Id: hal-00018964
https://hal.science/hal-00018964

Preprint submitted on 13 Feb 2006

Accurate Calculation of Mutual Inductance and Magnetic Fields in a Birdcage Coil

P. Boissoles and G. Caloz

February 13, 2006

Abstract

We present a detailed and complete analysis of a birdcage coil designed for MRI experiment through an equivalent circuit model. We derive analytic equations which can be used to predict a priori the full mutual inductances between conductors and the complete resonant spectrum for unshielded coils with high accuracy. The equations are valid for lowpass, highpass, and bandpass structures. We show that the approximation of a sinusoidal current pattern–which is usually used in the literature–is justified. Moreover, we reduce Neumann formula to the computation of two integrals and present an accurate algorithm to compute them. We also compute the magnetic field pattern of a birdcage coil. Our model is validated through numerical simulations which are compared to experimental results.

1 Introduction

Since their introduction over two decades ago, birdcage coils ([1, 2]) are often used in MRI experiments since they generate an adequate homogeneous radiofrequency magnetic field. Since then several studies have used the equivalent circuit method to predict the mutual inductances between conductors and the resonant spectrum. Hayes and al. ([1]) showed that a N leg coil has $N/2 + 1$ distinct resonant modes but didn't compare their results to effective experiment neither got numerical results. Tropp ([2, 3]) showed that couplings between near-neighbor meshes are dominant and neglected remote neighbors. Leifer ([4]) showed that another resonant mode, called the Helmholtz mode, exists. Thus a N leg coil has $N/2 + 2$ distinct resonant modes, including the Helmholtz mode.

Analytic formulas for the resonant modes are presented in [4, 5, 6], where mutual inductance formulas are the one studied in [7].

All the above mentioned articles are using the equivalent circuit presented in [1]. In particular they neglect the electric resistance of conductors and don't discuss tension sources. We also find papers where the authors are introducing more sophisticated models, but still based on the circuit approach, see [8]. Let us mention other models based on the Time-Domain Finite-Difference method ([9]) to calculate the radiofrequency field generated by the coil. With this approach we can only handle rough approximations of the complete device since we need to use a structured mesh of the domain, usually arcs and rings of the antenna are modelled by wires on edges of elements. Moreover we have no hope to get analytic formulas for the resonant modes and we shortcut the mutual inductance computation, which are precisely our two main goals with comparison to experimental data.

In our paper we are introducing a model close to the ones of [1] and [8]. We add the electric resistance of the conductors and the tension sources. By using the classical electrical network theory we get a system of ordinary differential equations which is solved explicitly when introducing resonant modes. Numerical simulations validate our model, justify the usual stationary approach (see [1]) and lead to a method giving a precise cartography of the B_1 field inside the birdcage.

More precisely the content and the organisation of the paper are the following.

Section 2 is devoted to the circuit analysis of the birdcage coil. First in section 2.1 we derive the general system of equations satisfied by the current of the endrings (see Eq. [10]). Since the different matrices introduced are all circulant matrices we can solve explicitly this system in the two configurations considered in section 2.2 which are the ones actually used in practice. Moreover we give the expression of the different resonant pulsations (see Eq. [15], Eq. [27], and Eq. [30]), which are the same as [1].

To have numerical values of these pulsations it is necessary to calculate mutual inductances. As usual we use Neumann formula (see Eq. [36]). We show in section 3.1 that this formula reduces to a simple integral which is well

computed by classical quadrature formulas. Then we are able to compare our resonant frequencies to experimental data. We consider three cases in section 3.2: two lowpass and one highpass structures. In section 3.3 we show that the hypotheses necessary to establish and solve Eq. [10] are satisfied in practical situations. To conclude we justify in section 3.4 the sinusoidal approach. We show that the transient state can be neglected in comparison with the stationary state.

Section 4 is devoted to numerical simulations of the radiofrequency field of the birdcage coil. We show numerically properties of the field corresponding to several resonant pulsations. Clearly the first mode is the only appropriate one for applications in MRI.

2 Birdcage Coil Circuit analysis

2.1 The equations

We consider a N leg bandpass birdcage coil with capacitors in both endrings and legs (see Fig. 1).
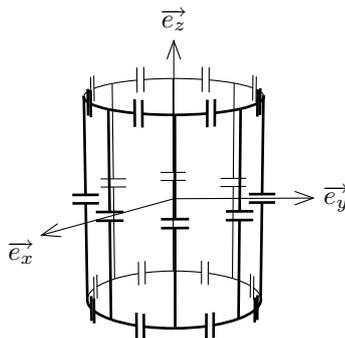

Figure 1: Bandpass birdcage coil

Our electric equivalent circuit is based on electrical network theory. We model each conductor as an inductance and a resistance. Thus the bandpass birdcage coil is described as the repetition of the electric network segment shown in Fig. 2, with left and right-most ends connected together.

In Fig. 2, L^{b} represents the self-inductance of a single leg, L^{a} the self-inductance of a single endring arc, C^{a} the capacitance of the capacitor between two legs and C^{b} represents the capacitance of the capacitor between two opposite endring arcs. This model includes the lowpass and highpass coils as special cases when $1/C^{\mathrm{a}}$ or $1/C^{\mathrm{b}}$ is set to zero. We also take into account mutual inductances: we note $L_{n,k}^{\mathrm{b}}$ the mutual inductance between the n-th and the k-th leg, $L_{n,k}^{\mathrm{a}}$ the mutual inductance between the n-th and the k-th endring segment in the same endring and $\overline{L_{n,k}^{\mathrm{a}}}$ the mutual inductance between the n-th and the k-th endring segment in opposite endring. For convenience, we define $L_{1,1}^{\mathrm{b}} = L^{\mathrm{b}}$ and

2

$L_{1,1}^{\mathrm{a}} = L^{\mathrm{a}}$. We note I_n^{b} the current in the n-th leg, I_n the current in the n-th arc of the top endring and J_n the current in the n-th arc of the bottom endring where n takes integer values. All over the paper the indices are taken modulo N so that, for example, $I_{N+n} = I_n$. Contrarily to what is usually assumed in the previous papers, here the currents I_n and J_n are general functions of the time t, not necessarily sinusoidal or equal.
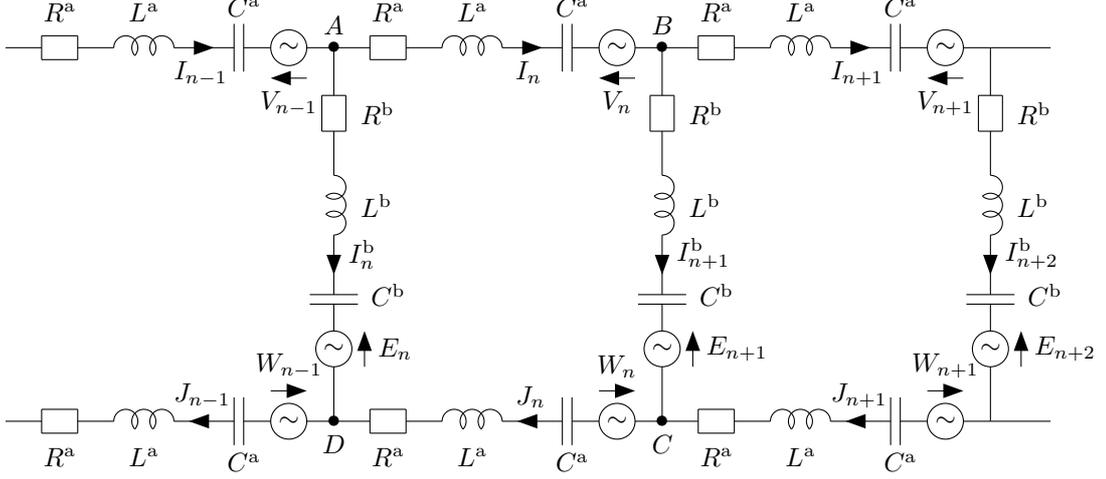

Figure 2: A section of the birdcage equivalent circuit

By applying the Kirchhoff law at the points A and D, we obtain:

$$\left\{ \begin{array}{l} \forall\, 1 \leqslant n \leqslant N,\ I_n^{\mathrm{b}} = I_{n-1} - I_n, \\ \forall\, 1 \leqslant n \leqslant N,\ J_n = J_1 - I_1 + I_n. \end{array} \right. \tag{1}$$

The Kirchhoff law on the mesh $ABCD$ gives the system of coupled equations

$$
\begin{aligned}
\forall\, 1 \leqslant n \leqslant N, \quad & \sum_{k=1}^{N} L_{n,k}^{\mathrm{a}}\, \frac{\mathrm{e}^2 I_k}{\mathrm{e}t^2} - \sum_{k=1}^{N} \overline{L_{n,k}^{\mathrm{a}}}\, \frac{\mathrm{e}^2 J_k}{\mathrm{e}t^2} + R^{\mathrm{a}}\, \frac{\mathrm{e}I_n}{\mathrm{e}t} + \frac{I_n}{C^{\mathrm{a}}} - \frac{\mathrm{e}V_n}{\mathrm{e}t} \\
& - \left[\sum_{k=1}^{N} L_{n,k}^{\mathrm{b}}\, \frac{\mathrm{e}^2 I_k^{\mathrm{b}}}{\mathrm{e}t^2} + R^{\mathrm{b}}\, \frac{\mathrm{e}I_n^{\mathrm{b}}}{\mathrm{e}t} + \frac{I_n^{\mathrm{b}}}{C^{\mathrm{b}}} + \frac{\mathrm{e}E_n}{\mathrm{e}t} \right] \\
& + \sum_{k=1}^{N} L_{n,k}^{\mathrm{a}}\, \frac{\mathrm{e}^2 J_k}{\mathrm{e}t^2} - \sum_{k=1}^{N} \overline{L_{n,k}^{\mathrm{a}}}\, \frac{\mathrm{e}^2 I_k}{\mathrm{e}t^2} + R^{\mathrm{a}}\, \frac{\mathrm{e}J_n}{\mathrm{e}t} + \frac{J_n}{C^{\mathrm{a}}} - \frac{\mathrm{e}W_n}{\mathrm{e}t} \\
& + \sum_{k=1}^{N} L_{n+1-k}^{\mathrm{b}}\, \frac{\mathrm{e}^2 I_k^{\mathrm{b}}}{\mathrm{e}t^2} + R^{\mathrm{b}}\, \frac{\mathrm{e}I_{n+1}^{\mathrm{b}}}{\mathrm{e}t} + \frac{I_{n+1}^{\mathrm{b}}}{C^{\mathrm{b}}} + \frac{\mathrm{e}E_{n+1}}{\mathrm{e}t} = 0.
\end{aligned}
\tag{2}
$$

The Kirchhoff law on the top endring mesh and on the bottom one leads to

$$\sum_{n=1}^{N} \left[\sum_{k=1}^{N} L_{n,k}^{\mathrm{a}}\, \frac{\mathrm{e}^2 I_k}{\mathrm{e}t^2} - \sum_{k=1}^{N} \overline{L_{n,k}^{\mathrm{a}}}\, \frac{\mathrm{e}^2 J_k}{\mathrm{e}t^2} + R^{\mathrm{a}}\, \frac{\mathrm{e}I_n}{\mathrm{e}t} + \frac{I_n}{C^{\mathrm{a}}} - \frac{\mathrm{e}V_n}{\mathrm{e}t} \right] = 0, \tag{3}$$

3

$$\sum_{n=1}^{N} \left[\sum_{k=1}^{N} L_{n,k}^{\mathrm{a}} \frac{\mathrm{e}^2 J_k}{\mathrm{e}t^2} - \sum_{k=1}^{N} \overline{L_{n,k}^{\mathrm{a}}} \frac{\mathrm{e}^2 I_k}{\mathrm{e}t^2} + R^{\mathrm{a}} \frac{\mathrm{e} J_n}{\mathrm{e}t} + \frac{J_n}{C^{\mathrm{a}}} - \frac{\mathrm{e} W_n}{\mathrm{e}t} \right] = 0. \qquad (4)$$

We easily verify that Eq. [4] is a consequence of Eq. [2] and Eq. [3]. Thus we have obtained $N+1$ equations for the $3N$ unknowns I_n, J_n, and I_n^{b}, $1 \leqslant n \leqslant N$.

Using Eq. [1], we substitute the unknowns I_n and J_1 to the unknowns J_2, ..., J_N and I_n^{b} in Eq. [2] and Eq. [3] to get:

$$\begin{aligned}
\forall\, 1 \leqslant n \leqslant N,\ & 2 \sum_{k=1}^{N} (L_{n,k}^{\mathrm{a}} - \overline{L_{n,k}^{\mathrm{a}}}) \frac{\mathrm{e}^2 I_k}{\mathrm{e}t^2} + 2 \left[R^{\mathrm{a}} \frac{\mathrm{e}}{\mathrm{e}t} + \frac{1}{C^{\mathrm{a}}} \right] I_n \\
& - \frac{\mathrm{e}(V_n + W_n)}{\mathrm{e}t} + \left[\sum_{k=1}^{N} (L_{n,k}^{\mathrm{a}} - \overline{L_{n,k}^{\mathrm{a}}}) \frac{\mathrm{e}^2}{\mathrm{e}t^2} + R^{\mathrm{a}} \frac{\mathrm{e}}{\mathrm{e}t} + \frac{1}{C^{\mathrm{a}}} \right] (J_1 - I_1) \\
& + \sum_{k=1}^{N} (L_{n+1,k}^{\mathrm{b}} - L_{n,k}^{\mathrm{b}}) \frac{\mathrm{e}^2 (I_{k-1} - I_k)}{\mathrm{e}t^2} \\
& + \left[R^{\mathrm{b}} \frac{\mathrm{e}}{\mathrm{e}t} + \frac{1}{C^{\mathrm{b}}} \right] (2 I_n - I_{n-1} - I_{n+1}) - \frac{\mathrm{e}(E_n - E_{n+1})}{\mathrm{e}t} = 0
\end{aligned} \qquad (5)$$

and

$$\begin{aligned}
\sum_{n=1}^{N} \left(\sum_{k=1}^{N} \left(L_{n,k}^{\mathrm{a}} - \overline{L_{n,k}^{\mathrm{a}}} \right) \right) \frac{\mathrm{e}^2 I_k}{\mathrm{e}t^2} - \left[\sum_{n=1}^{N} \sum_{k=1}^{N} \overline{L_{n,k}^{\mathrm{a}}} \right] \frac{\mathrm{e}^2 (J_1 - I_1)}{\mathrm{e}t^2} \\
+ \left(R^{\mathrm{a}} \frac{\mathrm{e}}{\mathrm{e}t} + \frac{1}{C^{\mathrm{a}}} \right) \sum_{n=1}^{N} I_n - \sum_{n=1}^{N} \frac{\mathrm{e} V_n}{\mathrm{e}t} = 0.
\end{aligned} \qquad (6)$$

Since the indices are taken modulo N,

$$\sum_{k=1}^{N} (L_{n+1,k}^{\mathrm{b}} - L_{n,k}^{\mathrm{b}}) I_{k-1} = \sum_{k=1}^{N} (L_{n+1,k+1}^{\mathrm{b}} - L_{n,k+1}^{\mathrm{b}}) I_k.$$

Finally I_n, $1 \leqslant n \leqslant N$, and J_1 are solutions of the system

$$
\left\{
\begin{aligned}
&\forall\, 1 \leqslant n \leqslant N, \\
&\sum_{k=1}^{N} \left[L_{n,k}^{\mathrm{b}} - L_{n+1,k}^{\mathrm{b}} - L_{n,k+1}^{\mathrm{b}} + L_{n+1,k+1}^{\mathrm{b}} + 2(L_{n,k}^{\mathrm{a}} - \overline{L_{n,k}^{\mathrm{a}}}) \right] \frac{\mathrm{e}^2 I_k}{\mathrm{e}t^2} \\
&\quad + 2(R^{\mathrm{a}} + R^{\mathrm{b}}) \frac{\mathrm{e}I_n}{\mathrm{e}t} - R^{\mathrm{b}} \frac{\mathrm{e}(I_{n-1} + I_{n+1})}{\mathrm{e}t} - \frac{1}{C^{\mathrm{b}}}(I_{n-1} + I_{n+1}) \\
&\quad + 2\left(\frac{1}{C^{\mathrm{a}}} + \frac{1}{C^{\mathrm{b}}} \right) I_n + \left[\sum_{k=1}^{N}(L_{n,k}^{\mathrm{a}} - \overline{L_{n,k}^{\mathrm{a}}}) \frac{\mathrm{e}^2}{\mathrm{e}t^2} + R^{\mathrm{a}} \frac{\mathrm{e}}{\mathrm{e}t} + \frac{1}{C^{\mathrm{a}}} \right] (J_1 - I_1) \\
&\quad = -\frac{\mathrm{e}(E_{n+1} - E_n)}{\mathrm{e}t} + \frac{\mathrm{e}(V_n + W_n)}{\mathrm{e}t}, \\
&\sum_{n=1}^{N} \left(\sum_{k=1}^{N} \left(L_{n,k}^{\mathrm{a}} - \overline{L_{n,k}^{\mathrm{a}}} \right) \right) \frac{\mathrm{e}^2 I_k}{\mathrm{e}t^2} - \left[\sum_{n=1}^{N} \sum_{k=1}^{N} \overline{L_{n,k}^{\mathrm{a}}} \right] \frac{\mathrm{e}^2 (J_1 - I_1)}{\mathrm{e}t^2} \\
&\quad + \left(R^{\mathrm{a}} \frac{\mathrm{e}}{\mathrm{e}t} + \frac{1}{C^{\mathrm{a}}} \right) \sum_{n=1}^{N} I_n = \sum_{n=1}^{N} \frac{\mathrm{e}V_n}{\mathrm{e}t}.
\end{aligned}
\right.
\tag{7}
$$

Since legs are all identical, Neumann formula in Eq. [36] shows that the mutual inductance between two legs depends only on their relative position, that is:

$$
\left\{
\begin{aligned}
&\forall\, 1 \leqslant n, k \leqslant N, \ L_{n,k}^{\mathrm{b}} = L_{k,n}^{\mathrm{b}}, \\
&\forall\, 1 \leqslant n, k, j \leqslant N, \ L_{n,k}^{\mathrm{b}} = L_{n+j,k+j}^{\mathrm{b}}, \\
&\forall\, 1 \leqslant n, k \leqslant N, \ L_{n,n+k}^{\mathrm{b}} = L_{n,n-k}^{\mathrm{b}}.
\end{aligned}
\right.
\tag{8}
$$

We suppose that all endring segments are identical so we have the same formulas for $L_{n,k}^{\mathrm{a}}$ and $\overline{L_{n,k}^{\mathrm{a}}}$.
We deduce from Eq. [8] that

$$
\forall\, 1 \leqslant n \leqslant N, \ \sum_{k=1}^{N} L_{n,k}^{\mathrm{a}} = \sum_{k=1}^{N} L_{k,n}^{\mathrm{a}} = \sum_{k=1}^{N} L_{1,k}^{\mathrm{a}}.
\tag{9}
$$

In order to obtain an equation for the only unknown $J_1 - I_1$, we sum the first N lines of Eq. [7] and subtract two times the last one:

$$
N \left[\sum_{k=1}^{N}(L_{1,k}^{\mathrm{a}} + \overline{L_{1,k}^{\mathrm{a}}}) \frac{\mathrm{e}^2}{\mathrm{e}t^2} + R^{\mathrm{a}} \frac{\mathrm{e}}{\mathrm{e}t} + \frac{1}{C^{\mathrm{a}}} \right] (J_1 - I_1) = -\frac{\mathrm{e}}{\mathrm{e}t} \sum_{n=1}^{N} (V_n - W_n).
$$

Finally we get the following system of ordinary differential equations:

$$
\begin{cases}
L\dfrac{e^2}{et^2}\begin{pmatrix} I_1 \\ \vdots \\ I_N \end{pmatrix} + R\dfrac{e}{et}\begin{pmatrix} I_1 \\ \vdots \\ I_N \end{pmatrix} + C\begin{pmatrix} I_1 \\ \vdots \\ I_N \end{pmatrix} \\[2em]
+\left[\displaystyle\sum_{k=1}^{N}(L_{1,k}^{\mathrm{a}} - \overline{L_{1,k}^{\mathrm{a}}})\dfrac{e^2}{et^2} + R^{\mathrm{a}}\dfrac{e}{et} + \dfrac{1}{C^{\mathrm{a}}}\right]\begin{pmatrix} J_1 - I_1 \\ \vdots \\ J_1 - I_1 \end{pmatrix} \\[2em]
\qquad\qquad = -\dfrac{e}{et}\begin{pmatrix} E_2 - E_1 \\ \vdots \\ E_1 - E_N \end{pmatrix} + \dfrac{e}{et}\begin{pmatrix} V_1 + W_1 \\ \vdots \\ V_N + W_N \end{pmatrix}, \\[2em]
N\left[\displaystyle\sum_{k=1}^{N}(L_{1,k}^{\mathrm{a}} + \overline{L_{1,k}^{\mathrm{a}}})\dfrac{e^2}{et^2} + R^{\mathrm{a}}\dfrac{e}{et} + \dfrac{1}{C^{\mathrm{a}}}\right](J_1 - I_1) = -\dfrac{e}{et}\displaystyle\sum_{n=1}^{N}(V_n - W_n),
\end{cases}
\tag{10}
$$

where L, R and C are $N \times N$ square matrices whose elements are given by:

$$
L_{n,k} = L_{n,k}^{\mathrm{b}} - L_{n+1,k}^{\mathrm{b}} - L_{n,k+1}^{\mathrm{b}} + L_{n+1,k+1}^{\mathrm{b}} + 2\left(L_{n,k}^{\mathrm{a}} - \overline{L_{n,k}^{\mathrm{a}}}\right), \tag{11}
$$

$$
R_{n,k} = 2\left(R^{\mathrm{a}} + R^{\mathrm{b}}\right)\delta_{n,k} - \delta_{n+1,k}R^{\mathrm{b}} - \delta_{n,k+1}R^{\mathrm{b}}, \tag{12}
$$

$$
C_{n,k} = 2\left(\dfrac{1}{C^{\mathrm{a}}} + \dfrac{1}{C^{\mathrm{b}}}\right)\delta_{n,k} - \dfrac{\delta_{n+1,k}}{C^{\mathrm{b}}} - \dfrac{\delta_{n,k+1}}{C^{\mathrm{b}}}, \tag{13}
$$

where $\delta_{n,k}$ is the Kronecker symbol, defined as: $\delta_{n,k} = 1$ for $n = k$ and $\delta_{n,k} = 0$ for $n \neq k$.

2.2 Resolution of the system of ordinary differential equations

We only consider the two cases:

- $\forall\, 1 \leqslant n \leqslant N,\ V_n = W_n$,
- $\forall\, 1 \leqslant n \leqslant N,\ V_n = -W_n$,

which cover the essential features encountered in the applications.

In the first case, the last line of Eq. [10] is

$$
\dfrac{e^2 y}{et^2} + \dfrac{1}{\tau_{\mathrm{CR}}}\dfrac{ey}{et} + \omega_{\mathrm{CR}}^2\, y = 0, \tag{14}
$$

where $y = J_1 - I_1$,

$$
\omega_{\mathrm{CR}} = \left(\sqrt{C^{\mathrm{a}}\sum_{k=1}^{N}(L_{1,k}^{\mathrm{a}} + \overline{L_{1,k}^{\mathrm{a}}})}\right)^{-1}, \tag{15}
$$

and

$$\tau_{\mathrm{CR}} = \frac{1}{R^{\mathrm{a}}} \sum_{k=1}^{N} (L_{1,k}^{\mathrm{a}} + \overline{L_{1,k}^{\mathrm{a}}}) \text{ is assumed to be strictly positive.} \qquad (16)$$

If $1/C^{\mathrm{a}} = 0$, that is in lowpass mode, the solutions of Eq. [14] are:

$$y(t) = A\mathrm{e}^{-t/\tau_{\mathrm{CR}}} + B \text{ with } A, B \in \mathbb{C}.$$

In the case $1/C^{\mathrm{a}} \neq 0$, we suppose moreover that

$$\Delta_{\mathrm{CR}} = \frac{1}{\tau_{\mathrm{CR}}^2} - 4\omega_{\mathrm{CR}}^2 < 0. \qquad (17)$$

The solutions of Eq. [14] are then:

$$y(t) = \mathrm{e}^{-t/2\tau_{\mathrm{CR}}}(A\cos(\omega_{\mathrm{CR}}^a t) + B\sin(\omega_{\mathrm{CR}}^a t)) \text{ where } A, B \in \mathbb{C} \text{ and}$$

$$\omega_{\mathrm{CR}}^a = \omega_{\mathrm{CR}} \sqrt{1 - \frac{1}{4\omega_{\mathrm{CR}}^2 \tau_{\mathrm{CR}}^2}}.$$

In both cases, the unique solution of the differential equation Eq. [14] with initial conditions $y(0) = y'(0) = 0$ is $y(t) = 0$, that is $J_1 = I_1$. Using Eq. [1] we obtain $I_n = J_n$, the usual assumption found in the literature (see [1], [4]). Then the system in Eq. [10] reduces to:

$$\begin{cases} L\dfrac{\mathrm{e}^2}{\mathrm{e}t^2}\begin{pmatrix} I_1 \\ \vdots \\ I_N \end{pmatrix} + R\dfrac{\mathrm{e}}{\mathrm{e}t}\begin{pmatrix} I_1 \\ \vdots \\ I_N \end{pmatrix} + C\begin{pmatrix} I_1 \\ \vdots \\ I_N \end{pmatrix} = -\dfrac{\mathrm{e}}{\mathrm{e}t}\begin{pmatrix} E_2 - E_1 - 2V_1 \\ \vdots \\ E_1 - E_N - 2V_N \end{pmatrix}, \\ J_1 = I_1, \\ \forall\, 1 \leqslant n \leqslant N,\ V_n = W_n. \end{cases}$$
$$(18)$$

We see from Eq. [12] and Eq. [13] that matrices R and C are circulant, that is $R_{i+1,j+1} = R_{i,j}$. By using Eq. [8], we can show that L is also a circulant matrix. So, they are codiagonalisable in the basis composed of the columns of F^* with

$$F_{i,j}^* = \frac{1}{\sqrt{N}} \left(\exp\left(\frac{2\mathrm{i}\pi}{N}\right)\right)^{(i-1)(j-1)}. \qquad (19)$$

Let ι_j, $j = 0, ..., N-1$, be the components of $(I_1, ..., I_N)^T$ in this basis and s_j, $j = 0, ..., N-1$, those of $(-(E_2 - E_1) + 2V_1, ..., -(E_1 - E_N) + 2V_N)^T$. The matrices L, R, and C are circulant, so we have the analytic expression of their eigenvalues (see [10]):

$$\lambda_k^L = \sum_{m=0}^{N-1} L_{1,m+1}\ \exp\left(\frac{2\mathrm{i}km\pi}{N}\right), \qquad (20)$$

$$\lambda_k^R = 2\left(R^{\mathrm{a}} + R^{\mathrm{b}}\left[1 - \cos\left(\frac{2k\pi}{N}\right)\right]\right) > 0, \qquad (21)$$

$$\lambda_k^C = 2\left(\frac{1}{C^{\mathrm{a}}} + \frac{1}{C^{\mathrm{b}}}\left[1 - \cos\left(\frac{2k\pi}{N}\right)\right]\right) \geqslant 0. \qquad (22)$$

7

In this new framework, the differential system in Eq. [18] reduces to the N equations

$$\forall\, 0 \leqslant j \leqslant N-1,\ \lambda_j^L \frac{\mathrm{e}^2 \iota_{j+1}}{\mathrm{e}t^2} + \lambda_j^R \frac{\mathrm{e}\iota_{j+1}}{\mathrm{e}t} + \lambda_j^C \iota_{j+1} = \frac{\mathrm{e}s_{j+1}}{\mathrm{e}t}. \tag{23}$$

We suppose that:

$$\forall\, 0 \leqslant j \leqslant N-1,\ \lambda_j^L > 0, \tag{24}$$

$$\forall\, 0 \leqslant j \leqslant N-1,\ \Delta_j = \frac{1}{\tau_j^2} - 4\omega_j^2 < 0. \tag{25}$$

Then, we can write Eq. [23] under the form:

$$\forall\, 0 \leqslant j \leqslant N-1,\ \frac{\mathrm{e}^2 \iota_{j+1}}{\mathrm{e}t^2} + \frac{1}{\tau_j} \frac{\mathrm{e}\iota_{j+1}}{\mathrm{e}t} + \omega_j^2 \iota_{j+1} = \frac{1}{\lambda_j^L} \frac{\mathrm{e}s_{j+1}}{\mathrm{e}t}, \tag{26}$$

where $\tau_j = \lambda_j^L / \lambda_j^R > 0$ and the resonant frequencies of birdcage coil ω_j are given by

$$\omega_j = \sqrt{\frac{\lambda_j^C}{\lambda_j^L}} = \sqrt{\frac{2}{\lambda_j^L} \left(\frac{1}{C^{\mathrm{a}}} + \frac{1}{C^{\mathrm{b}}} \left[1 - \cos\left(\frac{2j\pi}{N} \right) \right] \right)}. \tag{27}$$

Indeed, Eq. [26] is the classical differential equation of an RLC network and we know that there is a resonant phenomenon for ι_{j+1} at the pulsation ω_j.

Moreover, if $s_{j+1}(t) = S_{j+1} \cos(\omega t) + T_{j+1} \sin(\omega t)$, we can explicitly solve Eq. [26]. The solution which satisfies the initial condition $\iota_{j+1}(0) = \iota'_{j+1}(0)$ is:

$$\iota_{j+1}(t) = \mathrm{e}^{-t/2\tau_j}(A \cos(\omega_j^a t) + B \sin(\omega_j^a t)) + C \cos(\omega t) + D \sin(\omega t), \tag{28}$$

where

$$\omega_j^a = \omega_j \sqrt{1 - \frac{1}{4\omega_j^2 \tau_j^2}},$$

$$\begin{pmatrix} A \\ B \end{pmatrix} = \begin{pmatrix} -C \\ -\dfrac{1}{\omega_j^a} \left(\dfrac{C}{2\tau_j} + D\omega \right) \end{pmatrix},$$

$$\begin{pmatrix} C \\ D \end{pmatrix} = \frac{\omega}{\lambda_j^L \left((\omega^2 - \omega_j^2)^2 + \dfrac{\omega^2}{\tau_j^2} \right)} \begin{pmatrix} -(\omega^2 - \omega_j^2) T_{j+1} & + & \dfrac{\omega}{\tau_j} S_{j+1} \\ \dfrac{\omega}{\tau_j} T_{j+1} & + & (\omega^2 - \omega_j^2) S_{j+1} \end{pmatrix}.$$

We notice that this solution is composed of an oscillating term at the pulsation ω imposed by the source s_{j+1} and a transient term exponentially decreasing.

Let us consider now the second case, where $V_n = -W_n$. By summing the first N equations in Eq. [10] and using Eq. [8] and Eq. [9], we obtain:

$$\frac{\mathrm{e}^2 y}{\mathrm{e}t^2} + \frac{1}{\tau_{\mathrm{AR}}} \frac{\mathrm{e}y}{\mathrm{e}t} + \omega_{\mathrm{AR}}^2\, y = 0, \tag{29}$$

where, by analogy with the first case, we have set

$$y = \sum_{n=1}^{N} \left(I_n + J_n \right),$$

$$\omega_{\mathrm{AR}} = \sqrt{\dfrac{1}{C^{\mathrm{a}} \displaystyle\sum_{k=1}^{N}(L_{1,k}^{\mathrm{a}} - \overline{L_{1,k}^{\mathrm{a}}})}}, \qquad (30)$$

and we suppose:

$$\tau_{\mathrm{AR}} \;=\; \frac{1}{R^{\mathrm{a}}} \sum_{k=1}^{N}(L_{1,k}^{\mathrm{a}} - \overline{L_{1,k}^{\mathrm{a}}}) > 0, \qquad (31)$$

$$\Delta_{\mathrm{AR}} \;=\; \frac{1}{\tau_{\mathrm{AR}}^2} - 4\,\omega_{\mathrm{AR}}^2 < 0. \qquad (32)$$

The unique solution of Eq. [29] which satisfies the initial condition $y(0) = y'(0) = 0$ is the null function, that is Eq. [7] reduces to:

$$
\begin{cases}
\widetilde{L}\dfrac{\mathrm{e}^2}{\mathrm{e}t^2}\begin{pmatrix} I_1 \\ \vdots \\ I_N \end{pmatrix} + \widetilde{R}\dfrac{\mathrm{e}}{\mathrm{e}t}\begin{pmatrix} I_1 \\ \vdots \\ I_N \end{pmatrix} + \widetilde{C}\begin{pmatrix} I_1 \\ \vdots \\ I_N \end{pmatrix} = -\dfrac{\mathrm{e}}{\mathrm{e}t}\begin{pmatrix} E_2 - E_1 \\ \vdots \\ E_1 - E_N \end{pmatrix}, \\[4mm]
\left[\displaystyle\sum_{n=1}^{N}(L_{n,k}^{\mathrm{a}} + \overline{L_{n,k}^{\mathrm{a}}})\dfrac{\mathrm{e}^2}{\mathrm{e}t^2} + R^{\mathrm{a}}\dfrac{\mathrm{e}}{\mathrm{e}t} + \dfrac{1}{C^{\mathrm{a}}}\right]\displaystyle\sum_{n=1}^{N}I_n = \dfrac{\mathrm{e}}{\mathrm{e}t}\displaystyle\sum_{n=1}^{N}V_n, \\[4mm]
J_1 = I_1 - \dfrac{2}{N}\displaystyle\sum_{n=1}^{N}I_n, \\[4mm]
\forall\, 1 \leqslant n \leqslant N,\; V_n = -W_n,
\end{cases}
\qquad (33)
$$

$$\text{where} \quad
\begin{cases}
\forall\, 1 \leqslant j,k \leqslant N,\; \widetilde{L}_{j,k} = L_{j,k} - \dfrac{2}{N}\displaystyle\sum_{n=1}^{N}(L_{n,k}^{\mathrm{a}} - \overline{L_{n,k}^{\mathrm{a}}}), \\[4mm]
\forall\, 1 \leqslant j,k \leqslant N,\; \widetilde{R}_{j,k} = R_{j,k} - 2\dfrac{R^{\mathrm{a}}}{N}, \\[4mm]
\forall\, 1 \leqslant j,k \leqslant N,\; \widetilde{C}_{j,k} = C_{j,k} - \dfrac{2}{NC^{\mathrm{a}}}.
\end{cases}
$$

As in the first case we work in the basis composed of the columns of F^* (see Eq. [19]) and we note ι_j, $j = 0,...,N-1$, the components of $(I_1,...,I_N)^T$ in this basis. By using $\sum_{n=1}^{N} I_n = \sqrt{N}\iota_1$, we show that the first N equations of the system in Eq. [33] are equivalent to:

$$\forall\, 0 \leqslant j \leqslant N-1,\; \lambda_j^{\widetilde{L}}\dfrac{\mathrm{e}^2\iota_{j+1}}{\mathrm{e}t^2} + \lambda_j^{\widetilde{R}}\dfrac{\mathrm{e}\iota_{j+1}}{\mathrm{e}t} + \lambda_j^{\widetilde{C}}\iota_{j+1} = \dfrac{\mathrm{e}s_{j+1}}{\mathrm{e}t}, \qquad (34)$$

9

where $(v_1, ..., v_N)^T$ are the components of $(V_1, ..., V_N)^T$ and $(s_1, ..., s_N)^T$ those of $-M(E_1, ..., E_N)^T$ with:

$$M_{n,k} = \delta_{n,k} - \delta_{n+1,k} - \delta_{n,k+1}.$$

Since the first eigenvalue of M is zero, Eq. [34] with $j = 0$ reduces to $0 = 0$. The $N - 1$ other ones are the same as in the first case. The last equation of system in Eq. [33] is

$$\left[\sum_{n=1}^{N} (L_{n,k}^{\mathrm{a}} + \overline{L_{n,k}^{\mathrm{a}}}) \frac{\mathrm{e}^2}{\mathrm{e}t^2} + R^{\mathrm{a}} \frac{\mathrm{e}}{\mathrm{e}t} + \frac{1}{C^{\mathrm{a}}} \right] \iota_1 = \frac{\mathrm{e}v_1}{\mathrm{e}t}. \tag{35}$$

The analysis of this equation is similar to the one of Eq. [26]: we observe a resonant phenomenon at pulsation ω_{CR} with characteristic time $2\tau_{\mathrm{CR}}$.

3 Numerical simulations of the resonant modes

3.1 Calculation of birdcage inductances

The methods usually presented in the literature to compute mutual inductances are based on formulas given in [7]. The goal of this section is to show how to reduce the mutual inductance formula to a double integral, which can be computed then by quadrature rules.

The mutual inductance between two conductors $\mathscr{V}_1$ and $\mathscr{V}_2$ fed with a current density J_1 and J_2 is expressed by the following Neumann formula :

$$M_{1,2} = \frac{\mu_0}{4\pi I_1 I_2} \int_{\mathscr{V}_1} \int_{\mathscr{V}_2} \frac{\overrightarrow{J_1}(r) . \overrightarrow{J_2}(r')}{|r - r'|} dv dv', \tag{36}$$

where μ_0 is the vacuum permeability, I_j the total current in the conductor $\mathscr{V}_j$.

Assuming the strip thickness negligible and the current uniformly distributed, that is $J_1 = I_1 \overrightarrow{e_z}/w_b$, $J_2 = I_2 \overrightarrow{e_z}/w_b$, with w_b the strip width, then the mutual inductance $L_{n,k}^{\mathrm{b}}$ reduces to:

$$L_{n,k}^{\mathrm{b}} = \frac{\mu_0}{4\pi} \frac{R^2}{w_{\mathrm{b}}^2} \int_0^h \int_{\theta_n}^{\theta_n + w_{\mathrm{b}}/R} \int_0^h \int_{\theta_k}^{\theta_k + w_{\mathrm{b}}/R} \frac{d\theta d\theta' dz dz'}{\sqrt{2R^2(1 - \cos(\theta - \theta')) + (z - z')^2}} \tag{37}$$

where $\theta_k = 2(k-1)\pi/N$ and h represents the leg length.

By integration by parts in z and z', the previous expression reduces to the double integral:

$$L_{n,k}^{\mathrm{b}} = \frac{\mu_0}{4\pi} \frac{R^2}{w_{\mathrm{b}}^2} \int_{\theta_n}^{\theta_n + w_{\mathrm{b}}/R} \int_{\theta_k}^{\theta_k + w_{\mathrm{b}}/R} \left[-2\sqrt{2R^2(1 - \cos(\theta - \theta')) + h^2} \right.$$
$$+ 2\sqrt{2R^2(1 - \cos(\theta - \theta'))} + h \ln\left(h + \sqrt{2R^2(1 - \cos(\theta - \theta')) + h^2} \right)$$
$$\left. - h \ln\left(-h + \sqrt{2R^2(1 - \cos(\theta - \theta')) + h^2} \right) \right] d\theta d\theta'. \tag{38}$$

Using a similar method we obtain for the mutual inductance concerning the endring the following expression:

$$
\begin{aligned}
L_{n,k}^{a,\overline{a}} = \frac{\mu_0}{4\pi} \frac{R^2}{w_a^2} \int_{2(n-1)\pi/N}^{2n\pi/N} \int_{2(k-1)\pi/N}^{2k\pi/N} &\cos(\theta-\theta') \Bigg[2\sqrt{2R^2(1-\cos(\theta-\theta'))+Z^2} \\
-\sqrt{2R^2(1-\cos(\theta-\theta'))+(Z+w_a)^2} &- \sqrt{2R^2(1-\cos(\theta-\theta'))+(Z-w_a)^2} \\
&-2Z\ln\left(Z+\sqrt{2R^2(1-\cos(\theta-\theta'))+Z^2}\right) \\
+(Z+w_a)\ln\left(Z+w_a+\sqrt{2R^2(1-\cos(\theta-\theta'))+(Z+w_a)^2}\right)& \\
+(Z-w_a)\ln\left(Z-w_a+\sqrt{2R^2(1-\cos(\theta-\theta'))+(Z-w_a)^2}\right)& \Bigg] d\theta d\theta',
\end{aligned}
$$

(39)

where w_a is the width of the arc, $Z=0$ for $L_{n,k}^{\mathrm{a}}$, and $Z=L-w_\mathrm{a}$ for $\overline{L_{n,k}^{\mathrm{a}}}$.

To evaluate the integrals in Eq. [38] and Eq. [39] we use the Gauss quadrature rule exact for polynomials of degree up to seven. Indeed, Gauss formulas don't need the interval extremities and the singularity $\theta=\theta'=2\pi/N$ when $Z=0$ is avoided. To circumvent the singularities when $\theta=\theta'$ and $Z=0$, the subdivisions associated to θ and θ' are shifted: if β is the number of subdivisions associated to the first integral in θ, $\gamma=\beta+1$ is the number associated to the second.

3.2 Comparison to measurements

In our mutual inductance comparisons, we have used two birdcage coils. The first one is a 16 leg birdcage coil with a diameter of 8.9 cm and a length of 12.8 cm. The width of the strip is 1 cm for the ring and 0.635 cm for the legs. Strip conductors are fixed at 35 μm. Fig. 3 shows how the strips were sized for mutual inductance calculation. A capacitor $C^\mathrm{a}=180$ pF is used in each leg to form a highpass structure. The second structure is the same with $C^\mathrm{a}=0$ and
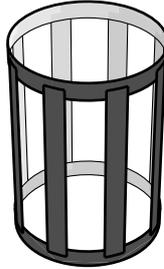

Figure 3: 3D view of birdcage coil

$C^\mathrm{b}=150$ pF to form a lowpass structure. We see in Fig. 3 that the leg length is $h=L-w_\mathrm{a}$. In our numerical simulation we have also used $h=L-2w_\mathrm{a}$. As we can see on tables 1 and 2, results are better in the second case. In the first case we take into account two times the inductance where leg and endring segments

Inductance	Measured (lowpass, nH)	Measured (highpass, nH)	$h = L - w_{\mathrm{a}}$ (nH)	$h = L - 2w_{\mathrm{a}}$ (nH)	[4] (nH)
$L_{1,1}$	117	115	124.802	114.847	122
$L_{1,2}$	-36.4	-34.9	-39.286	-35.641	-38.1
$L_{1,3}$	-5.3	-5.3	-5.847	-5.218	-6.1
$L_{1,4}$	-2.3	-2.3	-2.354	-2.085	-2.3
$L_{1,5}$	-1.4	-1.3	-1.394	-1.238	-1.4
$L_{1,6}$	-0.9	-0.8	-1.013	-0.908	-1.0
$L_{1,7}$	-0.9	-0.8	-0.836	-0.758	-0.8
$L_{1,8}$	-0.7	-0.8	-0.730	-0.689	-0.8
$L_{1,9}$	-0.8	-0.8	-0.754	-0.669	-0.7

Table 1: Computed and Measured Inductance

Inductance	Measured (lowpass) (nH)	$L - w_{\mathrm{a}}$ (%)	$h = L - 2w_{\mathrm{a}}$ (%)	[4] (%)
$L_{1,1}$	117	6.668	1.840	4.273
$L_{1,2}$	-36.4	7.930	2.084	4.670
$L_{1,3}$	-5.3	10.321	1.551	15.094
$L_{1,4}$	-2.3	2.366	9.363	0.0
$L_{1,5}$	-1.4	0.424	11.536	0.0
$L_{1,6}$	-0.9	12.515	-0.950	11.111
$L_{1,7}$	-0.9	7.126	15.783	11.111
$L_{1,8}$	-0.7	7.739	1.565	14.286
$L_{1,9}$	-0.8	8.737	16.395	12.500

Table 2: Relative error

are superposed. Since the thickness of the superposition is still negligible it is reasonable to take into account only once this inductance.

We also compare our method with respect to results obtained by [6]. The characteristics of the lowpass birdcage coil are:

$$\begin{cases} L = 12 \text{ cm}, R = 6.7 \text{ cm}, N = 8, \\ w_{\mathrm{a}} = w_{\mathrm{b}} = 1 \text{ cm}, \\ C^{\mathrm{b}} = 2 \text{ nF}, C^{\mathrm{a}} = 0 \text{ nF}. \end{cases} \qquad (40)$$

We collect in table 3 our results of resonant frequencies, those obtained in the references [6] and [11], and the measured values. For each mode we have reported the relative error between calculated value and measured value.

3.3   Justification of assumptions

Our goal now is to justify the hypotheses of section 2.2: Eq. [16], Eq. [17], Eq. [24], Eq. [25], Eq. [31], and Eq. [32]. For this, we need to compute the coefficient of the matrix L, that is the mutual inductance. As the analytic expressions of the mutual inductance and of the eigenvalues of L are cumbersome, it is

Mode	Measured (MHz)	$L - 2w_a$ (MHz)	Error (%)	[6] (MHz)	Error (%)	[11] (MHz)	Error (%)
1	8.081	8.095	0.178	8.259	2.203	9.290	14.961
2	12.075	12.187	0.928	12.044	0.257	12.383	2.551
3	13.875	14.036	1.161	13.695	1.297	13.718	1.131
4	14.475	14.574	0.686	14.174	2.079	14.475	2.501

Table 3: Birdcage (40) : frequencies

impossible to prove mathematically these assumptions. Nevertheless we have checked numerically their correctness. The method used to calculate the mutual inductance is exposed in section 3.1.

Let us consider the highpass structure presented in section 3.2. We obtain for the first line of matrix L:

$$(L)_1 = (114.8466 , -35.6413 , -5.2178 , -2.0846 , -1.2385 , -0.9086 ,$$
$$-0.7579 , -0.6890 , -0.6688 , -0.6890 , -0.7579 , -0.9086 ,$$
$$-1.2385 , -2.0846 , -5.2178 , -35.6413).$$

Thus

$$\sum_{m=1}^{N} \left(L_{1,m}^a - \overline{L_{1,m}^a} \right) = 10.5511 \times 10^{-9} > 0, \tag{41}$$

$$\sum_{m=1}^{N} \left(L_{1,m}^a + \overline{L_{1,m}^a} \right) = 10.9671 \times 10^{-9} > 0. \tag{42}$$

With Eq. [42] and Eq. [42] we check that the expressions in Eq. [15] and Eq. [30] are well defined.

In our numerical simulation, the resistance R^a and R^b are calculated with the formula:

$$R = \varrho \frac{L}{S} \text{ with } \begin{cases} L \text{ the conductor length in m,} \\ S \text{ its section in m}^2, \\ \varrho \text{ its electrical resistivity in } \Omega\text{m.} \end{cases} \tag{43}$$

We have used the resistivity of copper, that is $\varrho = 1.712 \times 10^{-8}$ Ωm. Then the computed characteristic values are:

$$\tau_{CR} = 1.283 \times 10^{-5} > 0, \Delta_{CR} = -2.026 \times 10^{18} < 0,$$
$$\tau_{AR} = 1.234 \times 10^{-5} > 0, \Delta_{AR} = -2.106 \times 10^{18} < 0.$$

We have also calculated the different τ_j and Δ_j:

$$(\tau_0, ..., \tau_{N-1}) = 10^{-4} \times (0.123 , 0.147 , 0.105 , 0.081 , 0.067 , 0.059 ,$$
$$0.054 , 0.052 , 0.051 , 0.052 , 0.054 , 0.059 , 0.067 , 0.081 , 0.105 , 0.147). \tag{44}$$

$$(\Delta_0, ..., \Delta_{N-1}) = -10^{18} \times (2.106 , 1.016 , 0.639 , 0.457 , 0.359 , 0.304 ,$$
$$0.271 , 0.254 , 0.249 , 0.254 , 0.271 , 0.304 , 0.359 , 0.457 , 0.639 , 1.016).$$

In conclusion all the hypotheses of section 2.2 are true: Eq. [16], Eq. [17], Eq. [24], Eq. [25], Eq. [31], and Eq. [32]. In particular, as a consequence of Eq. [24], the expression of ω_k in Eq. [27] is correctly defined.

We remark in Eq. [44] that: $\forall\, 1 \leqslant k \leqslant N-1,\ \tau_{N-k} = \tau_k$. It is a consequence of the symmetry satisfied by the eigenvalues λ_k^R and λ_k^L. Indeed, an immediate consequence of Eq. [21] is that:

$$\forall\, 1 \leqslant k \leqslant N-1,\ \lambda_{N-k}^R = \lambda_k^R, \tag{45}$$

$$\forall\, 1 \leqslant k \leqslant N-1,\ \lambda_{N-k}^L = \overline{\lambda_k^L}. \tag{46}$$

By using the relation $L_{1,m+1} = L_{1,N-m+1}$, we obtain:

$$\forall\, 1 \leqslant k \leqslant N-1,\ \lambda_{N-k}^L = \lambda_k^L. \tag{47}$$

We deduce from Eq. [46] and Eq. [47] that:

$$\forall\, 1 \leqslant k \leqslant N-1,\ \lambda_k^L \in \mathbb{R} \text{ and } \lambda_{N-k}^L = \lambda_k^L,$$

so $\tau_{N-k} = \lambda_{N-k}^L / \lambda_{N-k}^R = \lambda_k^L / \lambda_k^R = \tau_k$. We verify from Eq. [22] that $\lambda_{N-k}^C = \lambda_k^C$ so $\omega_{N-k} = \omega_k$ and an N leg birdcage coil has $N/2 + 2$ resonant frequencies: $N/2$ associated to $k = 1, ..., N/2,\ \omega_{\text{AR}} = \omega_0$ and ω_{CR}.

3.4   Validation of the sinusoidal approximation

To check that the sinusoidal approximation usually assumed in the literature is reasonable or not, we consider a spin-echo sequence. The emission time of the radiofrequency field is approximately $T = \pi/(4\pi \times 10^{-6}\omega_1) = 0.496$ ms long. Since $T/\tau_1 = 33.755$, the sinusoidal approximation is reasonable. To illustrate this, we represent in Fig. 4 the transient term and the complete courant ι_2 associated to the pulsation ω_1. Clearly the total current converges quickly to
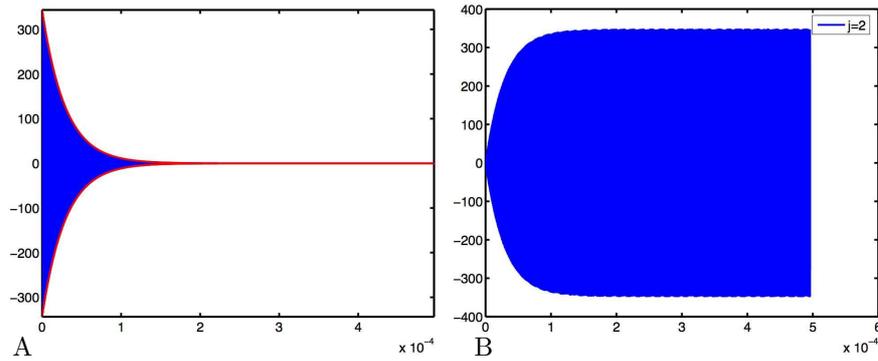

Figure 4: Transient (a) and total (b) current on $[0, T]$

the oscillating term. In conclusion we have shown that Eq. [48] and Eq. [49]

14

are "good approximation" of Eq. [18] and Eq. [33] where

$$\begin{cases} \omega^2 L \begin{pmatrix} I_1 \\ \vdots \\ I_N \end{pmatrix} + \mathrm{i}\omega R \begin{pmatrix} I_1 \\ \vdots \\ I_N \end{pmatrix} - C \begin{pmatrix} I_1 \\ \vdots \\ I_N \end{pmatrix} = -\mathrm{i}\omega \begin{pmatrix} E_2 - E_1 \\ \vdots \\ E_1 - E_N \end{pmatrix} + 2\mathrm{i}\omega \begin{pmatrix} V_1 \\ \vdots \\ V_N \end{pmatrix}, \\ J_1 = I_1, \\ \forall\, 1 \leqslant n \leqslant N,\ V_n = W_n, \end{cases}$$

(48)

$$\begin{cases} \omega^2 \widetilde{L} \begin{pmatrix} I_1 \\ \vdots \\ I_N \end{pmatrix} + \mathrm{i}\omega \widetilde{R} \begin{pmatrix} I_1 \\ \vdots \\ I_N \end{pmatrix} - \widetilde{C} \begin{pmatrix} I_1 \\ \vdots \\ I_N \end{pmatrix} = -\mathrm{i}\omega \begin{pmatrix} E_2 - E_1 \\ \vdots \\ E_1 - E_N \end{pmatrix}, \\ -\left[\omega^2 \sum_{k=1}^{N} (L_{1,k}^{\mathrm{a}} + \overline{L_{1,k}^{\mathrm{a}}}) + \mathrm{i}\omega R^{\mathrm{a}} - \frac{1}{C^{\mathrm{a}}} \right] \sum_{n=1}^{N} I_n = \mathrm{i}\omega \sum_{n=1}^{N} V_n, \\ J_1 = I_1 - \frac{2}{N} \sum_{n=1}^{N} I_n, \\ \forall\, 1 \leqslant n \leqslant N,\ V_n = -W_n. \end{cases}$$

(49)

4 B_1 field computation

From the previous sections, we know precisely the electric current in the birdcage coil conductors. Then we are able to compute the magnetic field patterns. Its expression outside the conductors is given by the Biot-Savart formula. To have in hand an efficient algorithm to compute the magnetic field, we still need to develop the different integrals. In particular the integrals coming from the endring segments contain elliptic integrals. A detailed analysis is given in [13]. All the results presented here are obtained with that method in the case of the first lowpass birdcage coil with 16 legs.

The diagrams in Fig. 5 refer to the magnetic field patterns in the plane perpendicular to the birdcage axis in its middle. In order to verify the magnetic
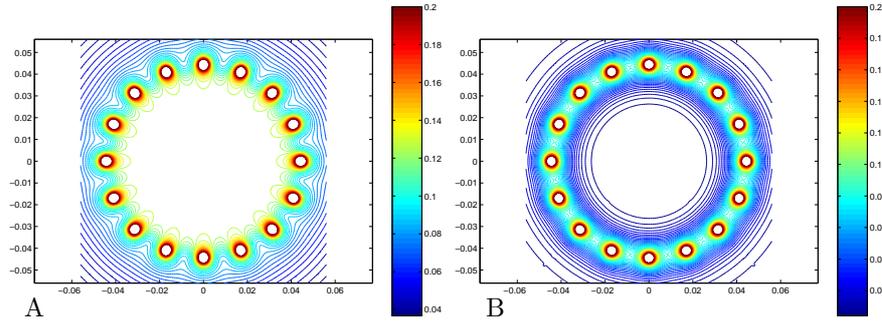

Figure 5: Module of B_1 field for mode 1 (a) and mode 8 (b)

field homogeneity and to justify the choice of the mode 1 in MRI, we plot the mode 1 field and the mode 8 field along the y axis on Fig. **??**. We remark that

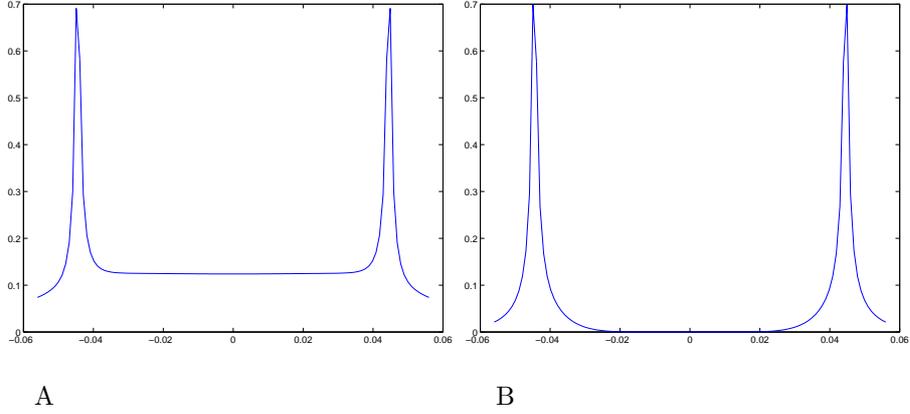A   B

Figure 6: Module of B_1 field for mode 1 (a) and mode 8 (b)

only the field associated to the mode 1 is not zero at the center of the birdcage coil. It is the only one with energy and homogeneity property in the center. That is why it is precisely the one used in MRI.

Remarque 4.1 *We plot only the mode 1 and the mode 8 because they are the two ones with the best homogeneity properties.*

On Fig. 7.a we have plotted the mode 1 magnetic field pattern in the plane of equation $y = 0$ containing the birdcage axis. We see the field still homogeneous at the center of the birdcage coil. More precisely, Fig. 7.b shows that in the area defined by a z coordinate between $-L/8 = -0.016$ cm and $L/8$ the mode 1 field is homogeneous.
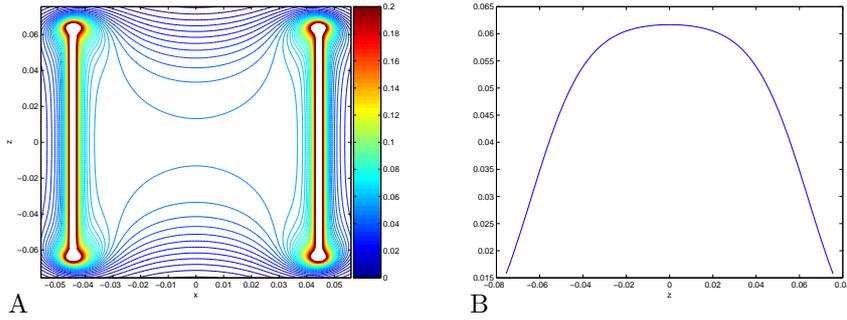

A   B

Figure 7: Norm of B_1 field for mode 1

16

5 Conclusion

We have developed a circuit based model to describe a birdcage coil with high accuracy. The analytic equations obtained for resonant frequencies and the corresponding radiofrequency field computation give a precise representation of the complete resonant spectrum and of the magnetic field pattern inside the coil. Moreover we give a rigorous and complete mathematical analysis of the model. We show also how the sinusoidal approximation is valid. We have compared our results with respect to experimental data and their are in good agreement. Finally we have developed reliable quadrature rules to compute the mutual inductances. All these results and much more can be found in the work [13].

References

[1] C. Hayes, W. Edelstein, J. Schenck, O. Mueller, M. Eash, An efficient, highly homogeneous radiofrequency coil for whole-body nmr imaging at 1.5 T, *J. Magn. Reson.* **63** (1985) 622–628.

[2] J. Tropp, The theory of the bird-cage resonator, *J. Magn. Reson.* **82** (1989) 51–62.

[3] J. Tropp, Mutual inductance in the bird-cage resonator, *J. Magn. Reson.* **126** (1997) 9–17.

[4] M. C. Leifer, Resonant modes of the birdcage coil, *J. Magn. Reson.* **124** (1997) 51–60.

[5] S. Li, C. M. Collins, B. J. Dardzinski, C. Chin, M. B. Smith, A method to create an optimum current distribution and homogeneous B_1 field for elliptical birdcage coils, *Magn. Reson. Med.* **37** (1997) 600–608.

[6] G. Giovannetti, L. Landini, M. F. Santarelli, V. Positano, A fast and accurate simulator for the design of birdcage coils in mri, *MAGMA* **15** (1-3) (2002) 36–44.

[7] F. W. Grover, *Inductance calculations, Working Formulas and Tables*, (Dover publications, 1946).

[8] F. D. Doty, G. J. Entzminger, C. D. Hauck, J. P. Staab, Practical aspects of birdcage coils, *J. Magn. Reson.* **138** (1999) 144–154.

[9] R. W. M. Lau, R. J. Sheppard, The modelling of biological systems in three dimensions using the time domain finite-difference method : I. the implementation of the model, *Phys. Med. Biol.* **31** (11) (1986) 1247–1256.

[10] P. J. Davis, *Circulant matrices*, (John Wiley & Sons, New York-Chichester-Brisbane, 1979, a Wiley-Interscience Publication, Pure and Applied Mathematics).

[11] J. Jin, *Electromagnetic Analysis and Design in Magnetic Resonance Imaging*, (CRC Press, 1997).

[12] Y. Chu, Numerical calculation for the magnetic field in current-carrying circular arc filament, *IEEE Transactions on magnetics* **34** (2) (1998) 502–504.

[13] P. Boissoles, *Problèmes mathématiques et numériques issus de l'imagerie par résonance magnétique nucléaire*, (PhD thesis, University of Rennes 1, France, 2005).